Coupled Thermal-Electromagnetic Model For Microwave Drilling

Uri Grosglik, Vladimir Dikhtyar, and Eli Jerby+
Faculty of Engineering, Tel Aviv Univesrity
Ramat Aviv 69978 ISRAEL
e-mail: jerby@eng.tau.ac.il, telefax: +972 3 640 8048

Abstract

The microwave drill is a novel method to drill into hard non-conductive materials by localized microwave energy. The microwave drill consists of a microwave source, a matched coaxial guide and a near-field concentrator. The latter focuses the microwave radiation into a small volume under the surface of the drilled material. The concentrator itself penetrates mechanically into the material via a hot spot created in a fast thermal runaway process. The microwave drill is applicable to a variety of materials including concrete, silicon, ceramics (in both slab and coating forms), rocks, glass, plastic, and wood. This paper presents a theoretical model for the coupled thermal-electromagnetic phenomena involved in the microwave drill operation. The model couples Maxwell's equations with the heat equation by the dissipated electromagnetic power. The latter modifies the temperature-dependent dielectric properties of the material, and causes a hot spot in it. The numerical simulation employs the finite-difference time-domain (FDTD) method in a cylindrical symmetry. The computation is performed by MATLAB on a personal computer. The paper presents simulation results for microwave drilling in Alumina. This numerical model enables a better understanding of the phenomena involved in the microwave-drilling process, and it assists the design and analysis of new experimental devices.

1. Introduction

The microwave-drill invention has been disclosed recently [1, 2]. If materialized, it may join a variety of useful applications based on microwave-heating mechanisms [3,4]. The key principle of the microwave-drilling method is the concentration of the microwave energy into a small spot, much smaller than the microwave wavelength itself. This is done in the near field by a microwave concentrator, which is brought to a contact with the material to be drilled. The microwave energy localized underneath the material surface generates a small hot spot [5], in which the material becomes soften or even molten. The concentrator pin itself is then inserted into the molten hot spot and shapes its boundaries. Finally, the pin is pulled out from the drilled hole, and the material cools down in its new shape. The process does not require fast rotating parts, and it makes no dust and no noise.

A principle scheme of the microwave drill is shown in Fig. 1a. The device consists of a microwave source (typically a magnetron), a matched coaxial wave-guide, and a concentrator. The latter is configured to concentrate the microwave radiation onto a small region in the near field, inside the drilled material. The power density is sufficient to liquefy the material at this point. The center electrode is inserted then into this hot point and forming the hole. The inner surface of the melted hole solidifies after the radiation ceased and forms a glossy coating. An experimental demonstration of this effect in a concrete brick is shown in a crosscut view in Fig. 1b. This glass can be removed easily by mechanical means in order to increase the hole to its final shape.

The method is applicable to a wide range of materials. More specifically, the operation of the concentrator is most effective when brought into close proximity, and preferably into contact, with a material of which the dielectric loss factor ε'' increases with temperature. This results in an enhanced coupling effect in which the microwave power absorption is highly focused at the hot spot in the target region. This positive-feedback effect parallels the *thermal run-away* known to be highly problematic in microwave furnaces. Examples of materials exhibiting this property include, stone, rock, marble, silicates ceramics, alumina, concrete, bricks of various kinds, basalt, plastics, wood, and cellulose based materials. The method is particularly significant in its ability to drill by localized melting of materials with melting temperatures over 1500^0C as verified in our experiments and simulations.

The microwave drill is effective for drilling and cutting in a variety of hard non-conductive dielectric materials, but not in metals. The latter reflect the radiation and therefor are almost not affected by the microwave drill. Hence, the microwave drill enables a distinction between different materials, and in particular between dielectrics and metals. Specifically, the microwave drill can be implemented to make holes and grooves in dielectric coatings on metallic substrates with no damage to the underlying metallic substrate.

The microwave drill can be implemented in relatively simple instruments, consuming moderate electrical powers. However, safety and RF interference considerations may limit its free public usage thus the microwave-drill concept is directed first for industrial manufacturing processes. This paper presents a numerical model [6] simulating the microwave drill operation.

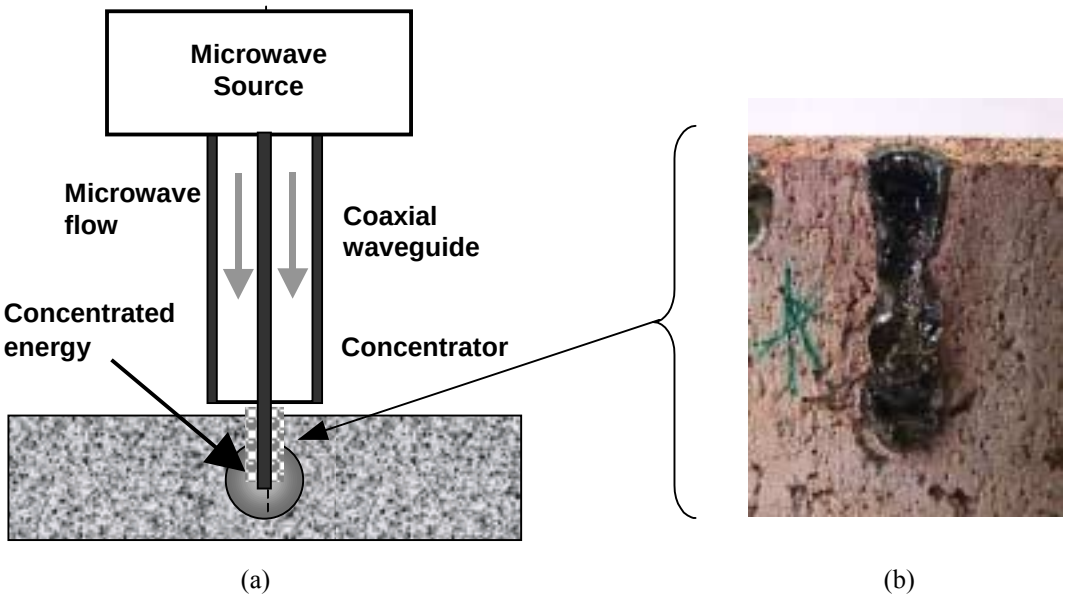

Fig. 1. (a) A simplified scheme of the microwave drill, and (b) its effect on concrete (the crosscut shows the glossy material before its removal).

2. Theory

The analysis of the microwave-drill operation couples together the electromagnetic (em) waves and the consequent thermal effect [7]. The dependence on temperature of the material dielectric properties is a key element in this analysis. Since the time scales of the em and thermal mechanisms are considerably different, a two-time-scale approach is adopted to simplify the solution of this problem. The em wave emitted by the concentrator and the power absorbed by the material in this region are described by Maxwell's equations for a lossy medium. In a cylindrical symmetry, these are given by

$$\frac{\partial H_\varphi}{\partial t} = \frac{1}{\mu_0}\frac{\partial E_z}{\partial r} - \frac{1}{\mu_0}\frac{\partial E_r}{\partial z}, \tag{1a}$$

$$\frac{\partial E_r}{\partial t} = -\frac{1}{\varepsilon_0 \varepsilon'}\frac{\partial H_\varphi}{\partial z} - \frac{\sigma_d}{\varepsilon_0 \varepsilon'} E_r, \tag{1b}$$

$$\frac{\partial E_z}{\partial t} = \frac{1}{\varepsilon_0 \varepsilon'}\frac{1}{r}\frac{\partial}{\partial r}\left(r H_\varphi\right) - \frac{\sigma_d}{\varepsilon_0 \varepsilon'} E_z, \tag{1c}$$

where E_r and E_z are the radial and longitudinal electric field components, respectively, H_φ is the azimuthal magnetic field component, σ_d is the dielectric conductivity. In the frequency domain, it represents the dielectric losses by $\sigma_d = \omega\varepsilon_0\varepsilon''$ where $\varepsilon = \varepsilon' - j\varepsilon''$ is the complex dielectric constant. In single-frequency steady-state conditions, the dissipated power density is given by

$$P_d = \sigma_d \left\langle |\mathbf{E}|^2 \right\rangle, \tag{2}$$

where $\langle K \rangle$ denotes the root-mean-square (RMS) of the total electric field in each point.

The heat equation employed to find the local temperature variation in a cylindrical symmetry is

$$\rho_m c_m \frac{\partial T}{\partial t} = k_t \left[\frac{1}{r}\frac{\partial}{\partial r}\left(r\frac{\partial T}{\partial r} \right) + \frac{\partial^2 T}{\partial z^2} \right] + P_d, \tag{3}$$

where ρ_m, c_m, and k_t are the density, specific heat, and thermal conductivity, respectively, of the medium, and T is the local temperature. Blackbody radiation effects are included in the boundry conditions as described below. The temperature dependence of the medium properties (ρ_m, c_m, k_t) is incorporated if available.

3. Numerical Model

The algorithm developed in this study consists of two numeriacl solvers, one for the em-wave equations (1,2) and the other for the heat equation (3). The em-wave solver treats the magnetic field component first and uses it for the solution of the electric field component. Then, the em power dissipated in the dielectric material is calculated, and provides the input for the solution of the heat equation. The dissipated power depends on the dielectric constant value, which depends in turn on temperature. The dielectric constant is calculated in each computation cycle, taking into account the actual local temperature.

The numerical solution is performed by the finite-difference-time-domain (FDTD) method [8,9]. Eq. (1c), for instance, in an elaborated FDTD form is

$$E_z^{n+1}(i, j+\tfrac{1}{2}) = E_z^n(i, j+\tfrac{1}{2}) \left[\frac{1 - \dfrac{\varepsilon''}{2\varepsilon'}\omega\Delta t}{1 + \dfrac{\varepsilon''}{2\varepsilon'}\omega\Delta t} \right] + \left[\frac{\dfrac{1}{\varepsilon_0\varepsilon'}\dfrac{\Delta t}{r(i, j+\frac{1}{2})\Delta r}}{1 + \dfrac{\varepsilon''}{2\varepsilon'}\omega\Delta t} \right] \cdot \left[r(i+\tfrac{1}{2}, j+\tfrac{1}{2}) H_\varphi^{n+\frac{1}{2}}(i+\tfrac{1}{2}, j+\tfrac{1}{2}) - r(i-\tfrac{1}{2}, j+\tfrac{1}{2}) H_\varphi^{n+\frac{1}{2}}(i-\tfrac{1}{2}, j+\tfrac{1}{2}) \right] \tag{4}$$

where Δt and n are the time step size and index, respectively, i and j are the radial and axial indices, respectively, and Δr and Δz are their corresponding step sizes.

The input for the thermal solver is the dissipated power density. The em power per unit volume is defined at the center of each unit cell, namely at the temperature node. The electric-field RMS values at these nodes are found by interpolations. The discrete form of the heat equation (3) is

$$T_{(i,j)}^{n+1} = T_{(i,j)}^n + \alpha D_t \left\{ \frac{\Delta t}{\Delta r^2} \left[T_{(i+1,j)}^n - 2T_{(i,j)}^n + T_{(i-1,j)}^n + \frac{1}{(i-0.5)} \left(T_{(i+1,j)}^n - T_{(i,j)}^n \right) \right] + \frac{\Delta t}{\Delta z^2} \left[T_{(i,j+1)}^n - 2T_{(i,j)}^n + T_{(i,j-1)}^n \right] + \frac{\Delta t}{k_t} P_d^n(i,j) \right\} \tag{5}$$

where $D_t = k_t / \rho_m c_m$, and $\alpha = \tau_{HEAT} / \tau_{EM}$ is the ratio between the computation time cycles of the heat and wave equations ($\alpha \sim 40 - 80$).

The microwave-drill workload dissipates heat in two mechanisms. One is the heat conduction through the surface boundaries, and the other is by heat radiation. The latter is dominant in the hot surface region near the concentrator. The heat flux dissipated by conduction is given by $q_{cond} = h_f (T - T_a)$ [10], where h_f is the convective heat-transfer coefficient, and T_a is the ambient temperature. The heat (blackbody) radiation is given by $q_{rad} = \sigma\varepsilon(T^4 - T_a^4)$ where σ is the Stephan-Boltzman constant and ε is the radiation emissivity. Both terms, for the heat conduction and radiation losses, are subtracted from the $P_d^n(i, j)$ term in Eq. (5) on the relevant boundaries.

4. Simulation Example

The numerical model of the microwave drill is demonstrated here by a simulation example of Alumina. Referring to Fig. 1a, the geometrical dimensions are as follows. The inner and outer diameters of the coaxial waveguide are 3mm and 16mm, respectively, (i.e. a 100 Ω impedance), its length is 120mm, and its inner electrode is inserted 6 mm into the Alumina slab.

The temperature dependence of the dielectric properties of Alumina are demonstrated in Figs. 2 by the imaginary part of its dielectric constant at 2.45 GHz [11]. Its real part varies in this temperature range from 9.2 to 10.5.

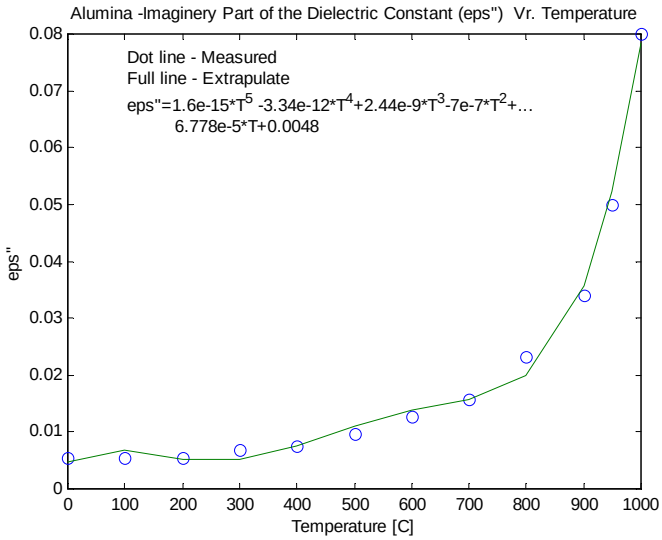

Fig. 2. The imaginary part of the dielectric constant of Alumina vs. temperature.

The simulation results in this case are shown here for a 22.5 kW RF input (note that much lower power levels down to 1 kW are applicable as well for correspondingly longer operating times). The total electric field magnitude in the coaxial waveguide and in the concentrator area is shown in Fig. 3 after 15 em-wave cycles (1200 computation cycles).

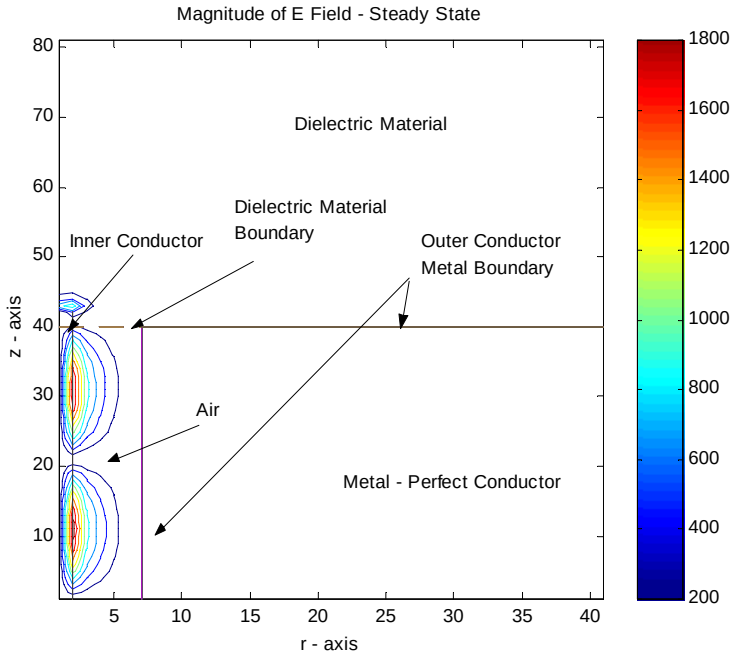

Fig. 3. Contour presentation of the total electric field [in V/m] after 15 cycles of the EM wave

The concentrator effect seems even more significant in Fig. 4, which shows the localization of the axial component of the electric field (i.e. $|E_z|$) in front of the concentrator..

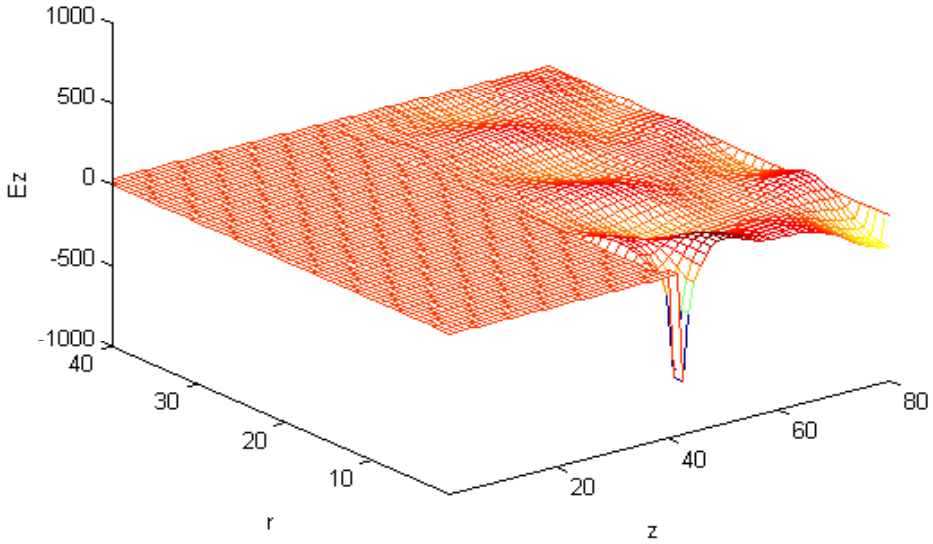

Fig. 4. The axial electric field component $|E_z|$ localized in front of the concentrator.

The evolution of the temperature in front of the concentrator pin during the microwave illumination is shown in Fig. 5. The result shows a relatively slow increase in temperature below 1000°C, but in higher temperatures a rapid growth is observed in accordance with the known thermal run-away effect. Unlike productive material processing methods in which the thermal runaway effect is harmful, the microwave drill makes use of it for local melting of hard materials in the microwave-drilling process.

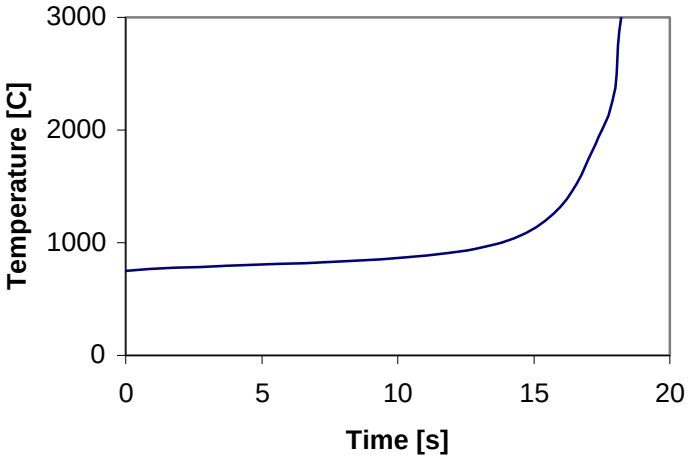

Fig. 5. The temperature vs. time simulation result in front of the concentrator pin.

5. Discussion

This paper presents preliminary results of the microwave-drill FDTD simulation. Further numerical studies are needed on other materials, and in comparison with the microwave-drill experiments. After its validation, this simulation could be useful for the design and analysis of microwave-drill experimental devices. A proper use of this simulation requires data on the temperature dependence of the dielectric properties as given in [12]. However, the microwave drill itself can be used as a diagnostic tool with its numerical simulation to assess material properties at high temperatures.

References

[1] E. Jerby and V. Dikhtyar, 'Method and device for drilling, cutting, nailing and joining solid non-conductive materials using microwave radiation," US Patent 6,114,676, Sept. 2000.

[2] E. Jerby and V. Dikhtyar, "Drilling into hard non-conducting materials by a localised microwave radiation," 8th Ampere Microwave Heating Conference, Sept. 2001 Bayreuth, Germany.

[3] A. C. Metaxas, "Foundations of electroheat – a unified approach," *Wiley*, Chichester, 1996.

[4] J. Thuery, "Microwave: industrial, scientific, and medical applications," *Artech House*, Boston, 1992.

[5] C.A. Vriezinga, "Thermal runaway in microwave heated isothermal slabs, cylinders, and spheres," J. Appl. Phys., Vol.83, pp.438-442, 1998.

[6] U. Grosglik, "FDTD simulation of the microwave drill," M.Sc. thesis, Faculty of Engineering, Tel Aviv University, 2002.

[7] Y. Alpert and E. Jerby, "Coupled thermal-electromagnetic model for microwave heating of temperature-dependent dielectric media," IEEE Trans. Plasma Science, Vol. 27, pp. 555-562, 1999.

[8] L. Ma, D.L. Paul, "Experimental validation of combined electromagnetic and thermal FDTD model of microwave heating process," IEEE Trans. Microwave Theory and Tech. Vol.43, pp. 2565-2570, 1995.

[9] F. Torres and B. Jecko, "Complete FDTD analysis of microwave heating process in frequency dependent and temperature dependent media," IEEE Trans. Microwave Theory and Tech., Vol. 45, pp.108-116, 1997.

[10] F.P. Incropera and D.P. Dewitt, "Fundamentals of heat and mass transfer" *Wiley*, NY, 1985.

[11] N.G. Evans and M.G. Hamlyn, "Microwave firing at 915MHz – efficiency and implications," Mat. Res. Soc. Symp. Proc., Vol. 430, pp. 9-13,1996.

[12] R.M. Hutcheon, J. Mouris and C.A. Pickles," Measurements of the complex dielectric constants of goethite and limonite minerals and nickel rich laterite ores at temperature up to 1150K in Air for frequencies 912 MHz and 2.46GHz," Microwave Properties North, Deep River, Ontario, Canada, 1999.